Extreme Fluorescence Sensitivity of Some Aniline Derivatives to Aqueous and Nonaqueous Environments: Mechanistic Study and Its Implication as a Fluorescent Probe

Juro Oshima,[†] Satoru Shiobara,[†] Hideki Naoumi,[†] Shigeo Kaneko,[†] Toshitada Yoshihara,[†] Ashok K. Mishra,[‡] and Seiji Tobita*,[†]

Department of Chemistry, Gunma University, Kiryu, Gunma 376-8515, Japan, and Department of Chemistry, Indian Institute of Technology Madras, Chennai 600 036, India

Received: December 1, 2005; In Final Form: February 2, 2006

Effects of solvent water on the photophysical properties of a series of meta- and para-substituted anilines have been investigated by means of time-resolved fluorescence, transient absorption, and photoacoustic measurements. Some aniline derivatives exhibit extremely short fluorescence lifetime (τ_f) and small quantum yield (Φ_f) in water (e.g., $\tau_f = 45$ ps and $\Phi_f = 0.0019$ for *m*-cyanoaniline (*m*-ANCN) in H_2O), which is in marked contrast with their much larger values in nonaqueous solvents ($\tau_f = 7.3$ ns and $\Phi_f = 0.14$ for *m*-ANCN in acetonitrile). Photoacoustic and transient absorption measurements show that the remarkable fluorescence quenching of *m*-ANCN in water is attributed almost exclusively to fast internal conversion. The lifetime measurements of *m*-ANCN in H_2O/acetonitrile binary solvent mixtures reveal that the quenching is related to variation of hydrogen-bonding interactions between the amino group and water molecules and the conformational change of the amino group upon electronic excitation. Similar fluorescence quenching due to solvent water is also found for *N*-alkylated *m*-ANCNs. The drastic differences in the fluorescence intensity and lifetime of *m*-ANCNs under hydrophobic and hydrophilic environments and also the large solvent polarity dependence of the fluorescence band position suggest the possibility that they can be utilized as fluorescent probes for investigating the microenvironment of biological systems. In suspensions of human serum albumin (HSA) in water, remarkable enhancement of the fluorescence intensity and lifetime is observed for *m*-ANCN and its *N*-alkylated derivatives, demonstrating that *m*-ANCNs can be a candidate for novel fluorescent probe with small molecular size.

1. Introduction

The photophysical properties of aromatic amines in solution are often affected markedly by the nature of the solvent environment (polarity, hydrogen-bonding ability, hydrophobicity, pH, etc.). High emission efficiency of some aromatic amines such as aminocoumarins and rhodamines has been utilized for laser dyes, where the influence of the medium on the emission efficiency is of essential importance as an important factor to determine the laser efficiency. The effect of solvent on the nonradiative processes in laser dyes has been widely investigated,[1−12] because the rate of radiationless transitions, which compete with the radiative transititon, is a dominant factor to determine the emission efficiency of an excited molecule in solution.

7-Aminocoumarin dyes with a flexible dialkylamino group at the 7-position and a strong electron-withdrawing group at the 3- or 4-position exhibit significant fluorescence quenching with an increase of solvent polarity.[1,2] The formation of the so-called twisted intramolecular charge transfer (TICT) state[3,8,10] and a structural change of the amino group from a planar to a pyramidal configuration (open-closed umbrella-like motion (ULM) mechanism[4,11,12]) have been considered to explain the characteristic nonradiative deactivation mechanisms in excited aminocoumarins and rhodamines in polar media.

The fluorescence sensitivity of aromatic amines to the surrounding environment has been utilized as fluorescent probes for examining the microenvironment of biological substances.[13−15] Since pioneering works of Weber and Laurence[16] and Weber and Farris,[17] anilinonaphthalenesulfonate (ANS), 6-propionyl-2-(dimethylamino)naphthalene (PRODAN), and their related compounds have been widely used as environmentally sensitive fluorescent probes. The fluorescence of ANS is relatively strong in nonaqueous solvents but significantly quenched in water. This characteristic property has been utilized to use ANS as a probe for hydrophobic domains of liposome membrane and protein.[18,19] Various mechanisms for ANS fluorescence quenching due to water that have been suggested are as follows: photoionization from the fluorescent state,[20−22] intersystem crossing to the triplet state,[23,24] intramolecular charge transfer,[25,26] $S_1 \rightarrow S_0$ internal conversion governed by the energy gap law,[27] and specific solute−solvent interactions.[28−30] Usually two or more processes contribute to the nonradiative rate of ANS and each process may depend differently on environment. PRODAN and related compounds involve an electron donor and acceptor substituents at remote positions in the naphthalene ring. As a result, these molecules have a significant intramolecular charge transfer (ICT) character in the excited singlet state, and are particularly useful as a micropolarity probe.[13−15,31] The photophysical behavior of PRODAN derivatives has recently been investigated by Abelt and co-workers[32,33] with particular interest in the character of the ICT state.

Among a number of solvents, water plays a pivotal role as the most important medium because it constitutes an important medium in biological systems. In the course of our studies on

[†] Gunma University.
[‡] Indian Institute of Technology Madras.

10.1021/jp0570014 CCC: $33.50
Published on Web 03/22/2006

the excited-state proton-transfer reactions of a series of protonated anilines,[34−36] we noticed that some aniline derivatives exhibit extremely short fluorescence lifetimes (τ_f) in water (e.g., $\tau_f = 45$ ps for *m*-cyanoaniline, *m*-ANCN, in H_2O). In nonaqueous solvents such as acetonitrile and ethanol, the fluorescence lifetimes increased dramatically, demonstrating that solvent water induces very rapid radiationless transitions in the aniline derivatives. This finding prompted us to investigate the possibility of using the aniline derivatives as novel fluorescent probes. Since the monosubstituted anilines have much smaller molecular sizes as compared with conventional fluorescent probes,[13−15] they can probe biological systems without significant perturbations, i.e., with maintaining the intrinsic structures and functions of the biological systems.

In this paper, we report the photophysical properties of meta- and para-substituted anilines in water and in nonaqueous solvents, possible mechanisms of the water-induced fluorescence quenching observed in some aniline derivatives such as *m*-ANCN, and an application of the characteristic photophysical properties of *m*-ANCN and its *N*-alkylated compounds in water to fluorescence probes for human serum albumin (HSA).

2. Experimental Section

Aniline (AN; Kanto), *m*-trifluoromethylaniline (*m*-ANCF$_3$; Tokyo kasei), *m*-fluoroaniline (*m*-ANF; Aldrich), *m*-methylaniline (*m*-ANM; Tokyo kasei), *m*-methoxyaniline (*m*-ANMO; Aldrich), *p*-trifluoromethylaniline (*p*-ANCF$_3$; Tokyo kasei), and *p*-fluoroaniline (*p*-ANF; Aldrich) were purified by vacuum distillation. *m*-Cyanoaniline (*m*-ANCN; Aldrich), *m*-hydroxyaniline (*m*-ANOH; Tokyo kasei), *p*-cyanoaniline (*p*-ANCN; Tokyo Kasei), *p*-methylaniline (*p*-ANM; Tokyo kasei), *p*-methoxyaniline (*m*-ANMO; Aldrich), and *p*-hydroxyaniline (*p*-ANOH; Tokyo kasei) were purified by recrystallization from hexanes−ethanol mixed solvent followed by vacuum sublimation. Cyclohexane (CH; Aldrich, spectrophotometric grade) was used as received. Acetonitrile (MeCN; Kanto), ethanol (EtOH), and trifluoroethanol (TFE; Kishida) were purified by distillation. Deionized water was purified by using a Millipore (MILLI-Q-Labo). D_2O (Merck, >99.8%) was used as received. *N*-Methyl-*m*-cyanoaniline (*m*-MMCN), *N*,*N*-dimethyl-*m*-cyanoaniline (*m*-DMCN), *N*-ethyl-*m*-cyanoaniline (*m*-MECN), and *N*,*N*-diethyl-*m*-cyanoaniline (*m*-DECN) were synthesized according to the reported *N*-alkylation method of primary amines,[37] and purified by column chromatograpy. Fatty acid free HSA (Sigma) was used as received.

Absorption and fluorescence spectra were recorded on an UV/vis spectrophotometer (Jasco, Ubest-50) and a spectrofluorometer (Hitachi, F-4010), respectively. Fluorescence quantum yields were determined by comparing the integrated intensities of the fluorescence spectra with that of standard quinine bisulfate in 0.5 M aqueous sulfuric acid solution ($\Phi_f = 0.546$[38]) or aniline in cyclohexane ($\Phi_f = 0.17$[39]).

Nanosecond fluorescence lifetimes were measured with a time-correlated single-photon counting fluorimeter (Edinburgh Analytical Instrument, FL-900CDT). A nanosecond pulsed discharge lamp (pulse width ~1.0 ns; repetition rate 40 kHz) filled with hydrogen gas was used as the excitation light source. The solutions used in the nanosecond fluorescence lifetime measurements were degassed by freeze−pump−thaw cycles on a high vacuum line. Picosecond time-resolved fluorescence measurements were made by using a femtosecond laser system that was based on a mode-locked Ti:sapphire laser (Spectra-Physics, Tsunami; center wavelength 800 nm, pulse width ~70 fs, repetition rate 82 MHz) pumped by a CW green laser (Spectra-Physics, Millenia V; 532 nm, 4.5 W). The repetition frequency was reduced to 4 MHz by using a pulse picker (Spectra-Physics, model 3980), and the third harmonic (266 nm, fwhm ~250 fs) was used as the excitation source. The monitoring system consisted of a microchannel plate photomultiplier tube (MCP-PMT; Hamamatsu, R3809U-51) cooled to −20 °C and a single-photon counting module (Becker and Hickl, SPC-530). The fluorescence photon signal detected by the MCP-PMT and the photon signal of the second harmonic (400 nm) of the Ti:sapphire laser were used for the start and stop pulses of a time-to-amplitude converter in this system. The instrumental response function had a half-width of about 25 ps. The fluorescence time profiles were analyzed by deconvolution with the instrumental response function.

Photoacoustic (PA) measurements were made by using a XeCl excimer laser (Lambda Physik, Lextra 50, pulse width 17 ns, 308 nm) as the excitation source. An argon-saturated aqueous solution of the sample was irradiated by the laser beam after passing through a slit (0.5 mm width), so that the effective acoustic transit time was ca. 340 ns. The laser fluence was varied by using a neutral density filter, and the laser pulse energy was measured with a pyroelectric energy meter (Laser Precision, RJP-753 and RJ7620). The PA signal detected by a piezoelectric detector (panametrics V103, 1 MHz) was amplified by using a wide-band high-input impedance amplifier (panametrics 5676, 50 kHz, 40 dB) and fed to a digitizing oscilloscope (Tektronix, TDS-744). The temperature of the sample solution was held to ±0.02.

The nanosecond laser photolysis experiments were carried out by using the third harmonic of a Nd^{3+}:YAG laser. Details of the laser photolysis system were reported elsewhere.[40] The solutions used in the laser photolysis experiments were degassed by freeze−pump−thaw cycles on a high-vacuum line.

3. Results and Discussion

3.1. Fluorescence Lifetimes of Meta- and Para-Substituted Anilines in Water. The fluorescence decay curves of the aniline and its derivatives examined in this study followed single-exponential kinetics in water except for *m*-ANF. The fluorescence time profiles of AN, *m*-ANMO, and *m*-ANCN in H_2O are shown in Figure 1, and the fluorescence lifetimes (τ_f) of the aniline derivatives in water are summarized in Table 1 along with their spectral properties (absorption (λ_{max}^{abs}) and fluorescence (λ_{max}^{fluo}) maxima, and Stokes shifts ($\Delta\bar{\nu}$)), the pK_a values in the ground state, and the Hammett σ constants of the meta and para substituents involved in the aniline derivatives. It is noted that the fluorescence lifetimes of meta and para-substituted anilines in water are extremely sensitive to the type of substituent and also the substitution position with respect to the amino group on the aromatic ring. One can find a general trend that meta-substituted compounds (except for *m*-ANCF$_3$) give much shorter lifetimes compared to their corresponding para-substituted ones. In particular, *m*-ANCN exhibits extremely short lifetimes in water, suggesting that very efficient fluorescence quenching due to solvent water is involved in these compounds. Interestingly, the extent of the water-induced fluorescence quenching does not correlate with the electron donor or acceptor character of the substituent for the ground-state reactions which can be evaluated from the Hammett σ values; substitution of an hydrogen atom in aniline for an electron-withdrawing cyano group results in a drastic decrease in τ_f, but similar substitution for an electron-withdrawing CF_3 group exerts little influence on τ_f.

In Table 1, fluorescence lifetimes measured in both H_2O and D_2O are reported. The deuterium isotope effects on the τ_f value

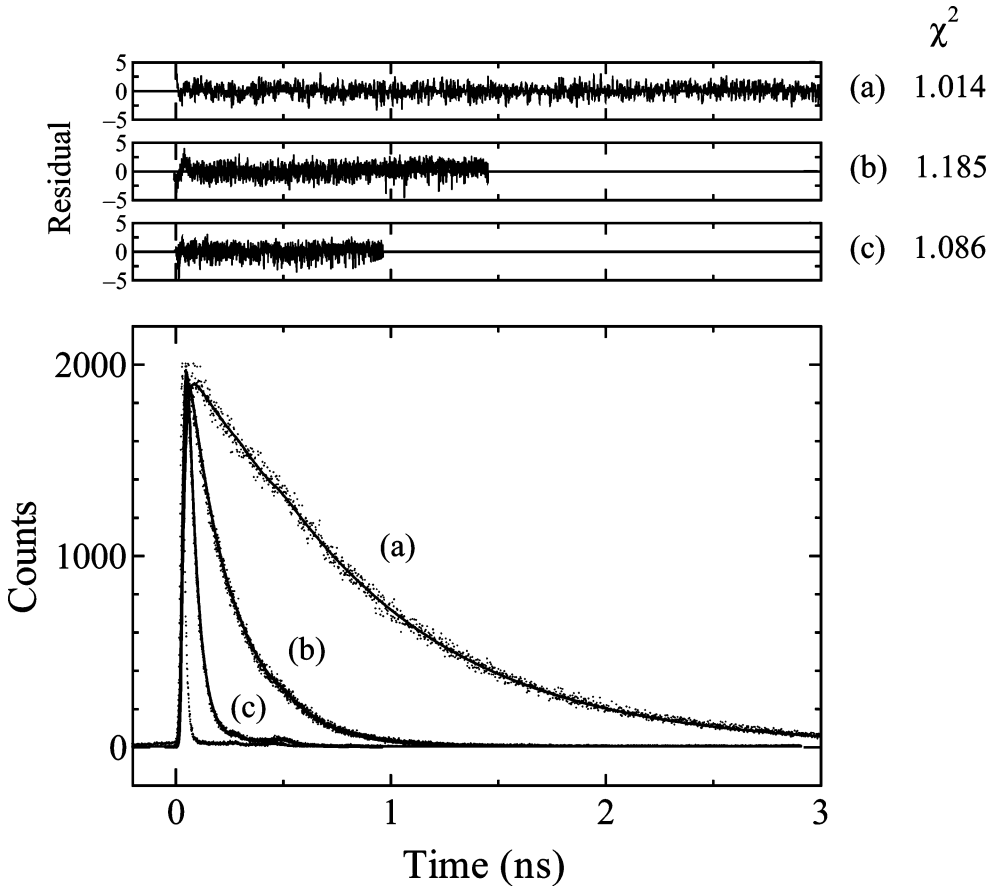

Figure 1. Fluorescence decay curves of (a) aniline, (b) *m*-ANMO, and (c) *m*-ANCN in H_2O at 293 K.

TABLE 1: Absorption (λ_{max}^{abs}) and Fluorescence (λ_{max}^{fluo}) Maxima, Stokes Shifts ($\Delta\bar{\nu}$), Fluorescence Lifetimes in H_2O ($\tau_f^{H_2O}$) and D_2O ($\tau_f^{D_2O}$) at 293 K, and Ionization Energy (IE*) in the S_1 State of Aniline and Meta- and Para-Substituted Anilines

compd	pK_a[a]	σ[b]	λ_{max}^{abs}/nm	λ_{max}^{fluo}/nm	$\Delta\bar{\nu}/10^3$ cm^{-1}	$\tau_f^{H_2O}$/ps	$\tau_f^{D_2O}$/ps	$\tau_f^{D_2O}/\tau_f^{H_2O}$	IE*/eV
AN	4.6	0.00	280	341	6.39	910	1420	1.6	3.71
m-ANCN	2.8	0.56	307	392	7.06	45	48	1.1	5.05
m-ANCF$_3$	3.5	0.43	289	359	6.80	1156	1130	1.0	
m-ANF	3.4	0.34	278	334	6.03	*c*	*c*	1.0	4.23
m-ANM	4.7	−0.07	282	341	6.13	205	418	2.0	3.50
m-ANMO	4.2	0.12	281	338	6.00	178	355	2.0	3.74
m-ANOH	4.4	0.12	282	337	5.79	101	233	2.3	3.47
p-ANCN	1.7	0.66	270	344	7.97	67	73	1.1	4.13
p-ANCF$_3$	2.6	0.54	280	340	6.30	955	956	1.0	
p-ANF	4.5	0.06	287	359	6.99	2400	2610	1.1	4.32
p-ANM	5.1	−0.17	286	351	6.48	526	1010	1.9	3.34
p-ANMO	5.3	−0.27	296	368	6.61	600	1290	2.2	3.68
p-ANOH	5.5	−0.37	297	375	7.00	420	1000	2.4	3.49

[a] pK_a values in the ground state. From ref 41. [b] Hammett constant. From ref 42. [c] The fluorescence decay curve of *m*-ANF in H_2O was best fitted by three decay components with lifetimes of 1.78 (5%), 95 (16%), and 908 ps (79%) ($\chi^2 = 1.077$).

can be seen for the compounds with an electron-donating group such as ANM and ANMO, i.e., the lifetime of these compounds in D_2O becomes longer by a factor of ca. 2.0, but the compounds with an electron-withdrawing group scarcely exhibit the isotope effect on the lifetimes. The existence of the deuterium isotope effect on τ_f of the aniline derivatives with an electron-donating group suggests that the O−H vibration of water molecules and/or N−H vibrations of the solute molecule are responsible for the water-induced fluorescence quenching in these compounds. There is little correlation between the τ_f in water and the ionization energy (IE*) for the excited singlet state, which was estimated by subtracting the 0−0 transition energy for $S_1 \leftarrow S_0$ transition from IE (ionization energy for the ground state). Therefore, quenching due to photoionization (electron photoejection), as suggested for 1,8-ANS,[20−22] does not appear to be an operating mechanism in the present systems. This can be confirmed by transient absorption measurements described below.

3.2. Solvent Effects on the Photophysical Properties of Meta- and Para-Substituted Anilines. For the compounds which show remarkably short fluorescence lifetimes in water, the fluorescence quantum yield and the fluorescence lifetime were measured in several organic solvents with different polarity and hydrogen-bonding ability (see Table 2). The Φ_f and τ_f values vary in an almost parallel way with the change of solvent, suggesting that the radiative rate is not affected significantly by the difference of solvent. The radiative (k_f) and nonradiative

TABLE 2: Absorption (λ_{max}^{abs}) and Fluorescence (λ_{max}^{fluo}) Maxima, Stokes Shifts ($\Delta\bar{\nu}$), Fluorescence Quantum Yield (Φ_f), Lifetime (τ_f), and Radiative (k_f) and Nonradiative (k_{nr}) Rate Constants of Anilines in Organic Solvents and H_2O at 293 K

compd	solvent	λ_{max}^{abs}/nm	λ_{max}^{fluo}/nm	$\Delta\bar{\nu}/10^3$ cm^{-1}	Φ_f	τ_f/ns	$k_f/10^7$ s^{-1}	$k_{nr}/10^8$ s^{-1}
AN	CH	288	316	3.08	0.17	4.3	3.9	1.9
	MeCN	290	332	4.36	0.13	3.6	3.6	2.4
	EtOH	286	337	5.29	0.15	3.2	4.7	2.7
	TFE	276	336	6.47	0.073	2.0	3.6	4.7
	H_2O	280	341	6.39	0.032	0.91	3.4	10
m-ANCN	CH	310	343	3.10	0.062	2.4	2.6	3.9
	MeCN	318	374	4.71	0.21	7.3	2.8	1.1
	EtOH	321	384	5.11	0.19	6.2	3.1	1.3
	TFE	300	380	7.00	0.0054	0.11	4.8	87
	H_2O	307	392	7.06	0.0019	0.045	4.4	230
p-ANCN	CH	263	323	7.06	0.13	5.6	2.4	1.6
	MeCN	272	338	7.18	0.14	3.3	4.4	2.6
	EtOH	276	341	6.91	0.041	0.68	6.0	14
	TFE	264	335	8.03	0.0052	0.13	4.0	77
	H_2O	270	344	7.97	0.0046	0.067	6.9	150
m-ANM	CH	289	317	3.06	0.19	4.8	4.0	1.7
	MeCN	290	332	4.36	0.15	3.6	4.1	2.3
	EtOH	287	337	5.17	0.14	3.0	4.5	2.9
	TFE	276	337	6.56	0.035	1.5	2.4	6.5
	H_2O	282	341	6.13	0.010	0.21	5.5	53
p-ANM	CH	294	326	3.34	0.17	3.7	4.6	2.3
	MeCN	297	341	4.34	0.17	3.9	4.3	2.1
	EtOH	291	347	5.55	0.13	3.3	4.0	2.7
	TFE	280	347	6.90	0.061	2.1	2.9	4.5
	H_2O	286	351	6.48	0.025	0.53	4.7	18
m-ANMO	CH	286	316	3.32	0.14	2.6	5.3	3.4
	MeCN	288	327	4.14	0.091	1.8	5.1	5.1
	EtOH	286	334	5.02	0.079	1.4	5.6	6.6
	TFE	276	337	6.56	0.0048	0.16	3.0	62
	H_2O	281	338	6.00	0.014	0.18	7.9	55
p-ANMO	CH	306	345	3.69	0.14	2.3	6.3	3.8
	MeCN	308	360	4.69	0.15	3.6	4.2	2.4
	EtOH	301	364	5.75	0.15	3.8	4.0	2.2
	TFE	289	364	7.13	0.094	2.9	3.3	3.2
	H_2O	296	368	6.61	0.040	0.60	6.7	16

(k_{nr}) rate constants were estimated by using the following relations:

$$k_f = \Phi_f/\tau_f \quad (1)$$

$$k_{nr} = (1 - \Phi_f)/\tau_f \quad (2)$$

It is noteworthy in Table 2 that the magnitude of the nonradiative rate constant in CH, MeCN, and EtOH does not vary significantly with the change of the solvent polarity except for *p*-ANCN in EtOH, and the marked quenching is seen only in strongly hydrogen-donating solvents TFE and H_2O. This clearly shows that there is no correlation between the fluorescence quenching and the solvent polarity and suggests that hydrogen-bonding interactions between solute and solvent molecules are related to the fluorescence quenching of the aniline derivatives in TFE and H_2O. Since the hydrogen-bonding donor ability of H_2O ($\alpha = 1.17$) evaluated from the Kamlet−Taft's solvatochromic parameter α[43,44] is smaller than that ($\alpha = 1.51$) of TFE, the extraordinarily large quenching effect of water is found to originate from a characteristic solvent property of water. As can be seen from Table 2, the nonradiative rate constants for *m*-ANCN and *p*-ANCN in water are extremely large (of the order of 10^{10} s^{-1}).

Although the influence of the substituted position on the τ_f of monosubstituted anilines in water exhibits similar features for the compounds in Table 1, the effect of the water solvent on τ_f does not simply correlate with particular physical parameters such as pK_a, σ, the Stokes shift $\Delta\bar{\nu}$, and IE* in the compounds. In particular, the fluorinated compounds show distinctly different characters as compared with the other compounds. The fluorescence decay curves of *m*-ANF do not conform to single-exponential kinetics and the contribution from photochemical reactions cannot be neglected in these compounds.[45,46] Recently Druzhinin et al.[47] have reported that the F-subsitution of 4-(azetidinyl)benzonitriles at ortho- or meta-position opens up an efficient internal conversion channel. These findings suggest that the water-induced quenching of the aniline derivatives in Table 1 cannot be explained on the basis of a common mechanism.

3.3. Nonradiative Deactivation Mechanism of the Excited Singlet State of *m*-ANCN in Water. To get an insight into the mechanism of the fluorescence quenching of the aniline derivatives due to solvent water, we examined the photophysical properties of *m*-ANCN, which showed the most remarkable fluorescence quenching in water, in more detail. Since the photophysical behavior of *m*-ANCN is analogous to that of ANS, we considered quenching mechanisms similar to those suggested in ANS: (1) photoionization, (2) intersystem crossing, (3) intramolecular charge transfer, (4) conformational changes of the amino group, and (5) specific solute−solvent interactions. Among these processes, the contribution of photoionization to fluorescence quenching is considered to be negligibly small because of the relatively high ionization energy of *m*-ANCN in the S_1 state (see Table 1) and the fact that no transients resulting from the photoionization process were observed for *m*-ANCN in water.

Internal Conversion and Intersystem Crossing. The UV irradiation experiment of *m*-ANCN in water showed that the contribution of photochemical reactions in the relaxation processes of *m*-ANCN in the S_1 state is negligibly small. Since

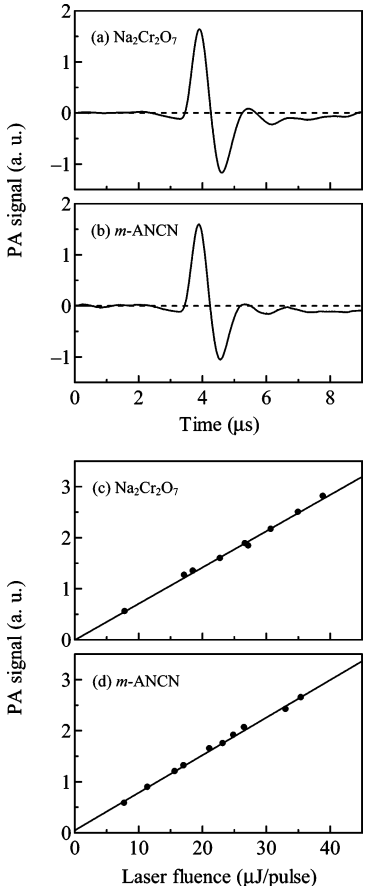

Figure 2. Photoacoustic signals for (a) the calorimetric reference $Na_2Cr_2O_7$ and (b) *m*-ANCN in Ar-saturated H_2O at 20.0 °C. The laser energy dependence of the PA signals of (c) $Na_2Cr_2O_7$ and (d) *m*-ANCN in Ar-saturated H_2O at 20.0 °C.

the fluorescence quantum yield of *m*-ANCN is extremely small ($\Phi_f = 0.0019$) in water, the dominant deactivation channels in water would be ascribed to intersystem crossing (ISC) to the T_1 state and/or internal conversion (IC) to the ground state. To distinguish the contribution of these processes to overall decay processes of the S_1 state, time-resolved photoacoustic (PA) measurements were carried out for *m*-ANCN in water.

The PA signal amplitude H produced after the absorption of a light pulse results basically from two processes occurring during the heat integration time:[48,49] thermally induced volume change in the solution ΔV_{th} and structural volume change ΔV_r,

$$H = k(\Delta V_{th} + \Delta V_r)$$

where k is an instrumental constant that depends on the geometrical arrangement and on some solution constants such as density ρ and sound velocity v_a. ΔV_{th} is the contraction or expansion of the solvent due to the heat released by nonradiative processes and given by

$$\Delta V_{th} = k'\alpha\left(\frac{\beta}{c_p\rho}\right)E_a$$

where α is the fraction of the absorbed energy released as thermal energy within the response time of the detector, β is the thermal expansion coefficient, c_p is the heat capacity of the solution, and E_a is the absorbed energy. For neat water, $\beta = 0$ at 3.9 °C.

Panels a and b of Figure 2 show the PA signals of photocalorimetric reference $Na_2Cr_2O_7$ and *m*-ANCN in water at 20.0 °C. At 3.2 °C no PA signal was observed for both compounds, indicating that the contribution of structural volume change to overall PA signal is negligibly small for *m*-ANCN in water. At 20.0 °C the difference between the first maximum and minimum in PA signal was taken as the signal amplitude H. The amplitude H of the PA signal is related to the incident laser pulse energy E_0 by

$$H = K\alpha E_0(1 - 10^{-A}) \tag{3}$$

where K is a constant that depends on the geometry of the experimental setup and the thermoelastic quantities of the medium, and A is the absorbance of the solution at the excitation wavelength. The relationship between PA signals and laser energy was linear within the range studied (Figure 2c,d). Thus, the energy-normalized PA amplitudes for the sample compound and reference (H_{20}^S and H_{20}^{ref}) at 20.0 °C are obtained from the slope of the linear plots in Figure 2c,d, and the α value can be determined from eq 4

$$\alpha = \frac{H_{20}^S}{H_{20}^{ref}} \tag{4}$$

With the exception of the decay of the excited triplet state, all other decay processes occur within the heat integration time (ca. 340 ns), so that the quantum yield of intersystem crossing Φ_{isc} can be obtained from the following relation:

$$\alpha = 1 - \frac{\Phi_f\langle E_S\rangle}{E_\lambda} - \frac{\Phi_{isc}E_T}{E_\lambda} \tag{5}$$

where E_λ is the excitation energy (= 388 kJ/mol at 308 nm), E_T is the triplet energy, and $\langle E_S\rangle$ is the average energy dissipated by fluorescence from the S_1 state.

From the slopes of the straight lines in Figure 2c,d, the α value for *m*-ANCN in H_2O was obtained to be 1.03 ± 0.05. This indicates that the Φ_{isc} value nearly equals zero and the fast deactivation channel from the excited singlet state of *m*-ANCN in H_2O can be attributed to internal conversion. Assuming the value of Φ_{ic} to be 1.0, the rate constant of the IC induced by water quenching is estimated to be 2.3×10^{10} s^{-1}.

The transient absorption spectrum obtained by 266 nm laser photolysis of *m*-ANCN in H_2O showed no appreciable absorption band in the wavelength range of 300−800 nm. This is in contrast with the transient absorption spectrum of aniline in water, which consists of a broad absorption band at around 720 nm due to hydrated electron, an absorption band at around 425 nm due to the aniline cation radical, and an absorption band extending to a near-ultraviolet region due to the triplet state.[50] For aniline in water it has been reported[50,51] that photoionization takes place from the nonrelaxed excited singlet state and the dominant deactivation process from the relaxed S_1 state (fluorescence state) is internal conversion. In *m*-ANCN in H_2O the photoionization process is completely absent for both nonrelaxed and relaxed S_1 states. This is probably due to an increased photoionization threshold in *m*-ANCN (see Table 1).

Quenching in Water/Acetonitrile Binary Solvent Mixtures. The fluorescence lifetime of *m*-ANCN (5×10^{-4}M) was measured in water/acetonitrile binary solvent mixtures. In Figure 3a, the reciprocal of the τ_f value is plotted against water concentration in the mixed solvent. Since the radiative rate constant k_f does not change appreciably when the solvent is changed from water to acetonitrile (see Table 2), the remarkable decrease of τ_f in water is attributable to enhancement in the IC

TABLE 3: Photophysical and Spectral Properties of *N*-Methylaniline (MMAN), *N*-Ethylaniline (MEAN), *N*,*N*-Dimethylaniline (DMAN), *N*,*N*-Diethylaniline (DEAN), and Their *m*-Cyano Derivatives in H_2O at 293 K

compd	pK_a[a]	λ_{max}^{abs}/nm	λ_{max}^{fluo}/nm	$\Delta\bar{\nu}/10^3$ cm^{-1}	Φ_f	$\tau_f^{H_2O}$/ps	k_f[c]/10^7 s^{-1}	k_{nr}[c]/10^8 s^{-1}
MMAN	4.9	281	351	7.10	0.032[b]	1160	3.4	8.3
MEAN	5.1	283	356	7.25	0.041[b]	1260	3.8	7.6
DMAN	5.2	290	365	7.09	0.042[b]	2200	2.4	4.3
DEAN	6.6	304	362	5.27	0.049[b]	2560	2.7	3.6
m-MMCN	2.9	318	412	7.17	0.0027	82	3.3	120
m-MECN	3.2	317	413	7.33	0.0029	90	3.2	110
m-DMCN	3.0	324	431	7.66	0.0053	257	2.1	39
m-DECN	4.4	344	435	6.08	0.0061	330	1.8	30

[a] From ref 41. [b] From ref 53. [c] The values calculated by taking photoionization processes from the nonrelaxed S_1 state into account (see ref 53).

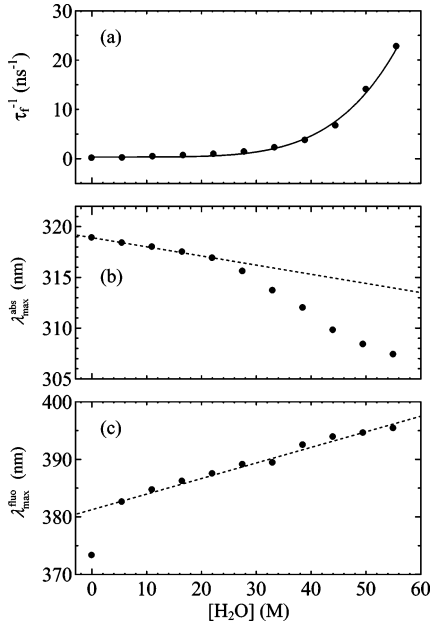

Figure 3. (a) The reciprocal of the fluorescence lifetime, (b) absorption maximum, and (c) fluorescence maximum as a function of water concentration in water/acetonitrile mixed solvent at 293 K.

rate, which can be approximated by the reciprocal of the τ_f value. With an increase of the water content in the mixed solvent, the IC rate increases gradually and a steep increase is seen from the concentration of about 30 M. In Figure 3b,c, the absorption and fluorescence maxima are also plotted against H_2O concentrations. It is noted that similar water concentration dependences are seen for τ_f^{-1} and λ_{max}^{abs}: the absorption maximum shifts to the blue almost linearly with increasing water concentration until about 20 M and more remarkable blue-shift begins from ~30 M. The involvement of aggregation at high water concentrations was examined by measuring the fluorescence decay of *m*-ANCN with different concentrations from 5.0×10^{-5} to 1.0×10^{-3} M in H_2O. The fluorescence decay curves followed single-exponential kinetics and constant lifetimes were obtained in this concentration range. Further, no significant change was observed for the absorption and fluorescence spectra. These observations show that aggregation at high water concentrations is not responsible for the fluorescence quenching. The increase in the blue shift from the water concentration of ~30 M suggests that specific solute−solvent interactions (hydrogen-bonding interactions) between the amino lone-pair electrons in *m*-ANCN and water molecules become remarkable from this concentration region. In contrast, the fluorescence maximum displays an almost linear change against the increase of the water concentration except that steep increase takes place from 0 to 5 M. This implies that the hydrogen bond formed in the ground state is completely broken in the fluorescent state, because in the excited singlet state an electron is migrated from the nitrogen lone pair to the aromatic system.[7,52] Such a change in the hydrogen bonding interactions in the excited state is supported from the fact that a significant increase in the acidity of protonated aniline in water occurs upon electronic excitation and *m*-cyano substitution of aniline enhances drastically the excited-state acidity of the protonated aniline.[36]

Effect of N-Alkylation on the Photophysical Properties of m-ANCN. *N*-Alkylation of *m*-ANCN increases greatly the fluorescence lifetime in water (see Table 3). Concomitant increases in Φ_f indicate that this results from reduction of the nonradiative rate with the alkylation of the amino group. Actually the nonradiative rate constant k_{nr} calculated from τ_f and Φ_f decreases substantially with *N*-alkylation. A similar tendency is also recognized for AN and its *N*-alkylated derivatives.[53] This finding also suggests the participation of hydrogen bonding interactions between the amino moiety and water molecules in the fast internal conversion process. It can be expected that there exist two different types of hydrogen bonding interactions between the amino group and water molecules for *m*-ANCN in water: an H-bond between the lone-pair electrons in the amino group and the O−H bond in water molecule, and that between the N−H bond in the amino group and the lone-pair electrons in the water molecule. The latter type of H-bond cannot be formed in *N*,*N*-dialkylated anilines, and the former type of H-bonding interactions would be weakened with *N*-alkylation of the amino group because of steric hindrance due to the bulky alkyl group(s).

It has been reported that alkylation of the amino group in aminobenzonitriles facilitates ICT reaction in the excited single state;[54] 4-(dialkylamino)benzonitriles exhibit a typical ICT emission in 1,4-dioxane, benzene, and even cyclohexane but the ICT state formation is not seen for 4-aminobenzonitrile and 4-(methylamino)benzonitrile in the same solvents. Thus, the reduction of the water-induced quenching by *N*-alkylation of *m*-ANCN and AN and also lack of appreciable fluorescence quenching in polar acetonitrile suggest that the water-induced quenching is not due to relaxation to an ICT state.

The amino nitrogen of aniline in the ground state possesses sp^3-like configuration with almost pyramidal structure, while upon electronic excitation the configuration of the amino group changes to sp^2-like with a more planar structure.[55,56] Such a structural change of the amino group in the S_1 state results in charge migration from the amino group to the benzene ring, leading to enhancement of the acidity of its protonated form in the excited state. In fact we have recently found that protonated aniline and protonated *m*-ANCN in aqueous solution undergo very fast excited-state proton dissociation.[34−36] In *m*-ANCN, intramolecular charge transfer from the amino group to the aromatic moiety in the S_1 state is enhanced by the presence of the cyano group, which may promote the break of the hydrogen bond between the amino group and the water molecule.

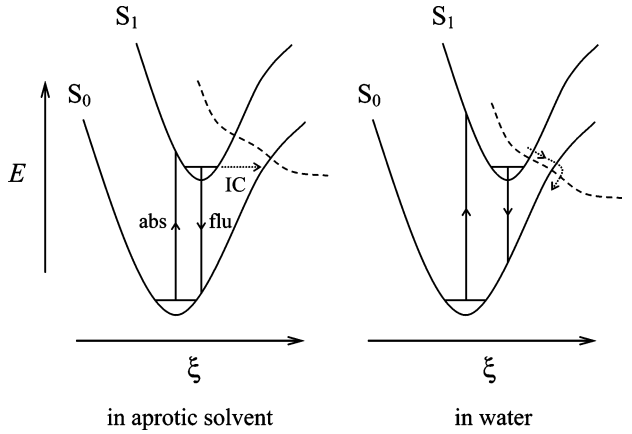

Figure 4. Schematic illustration of the deactivation pathways of *m*-ANCN in solution. The reaction coordinate involves the structural change of the amino group.

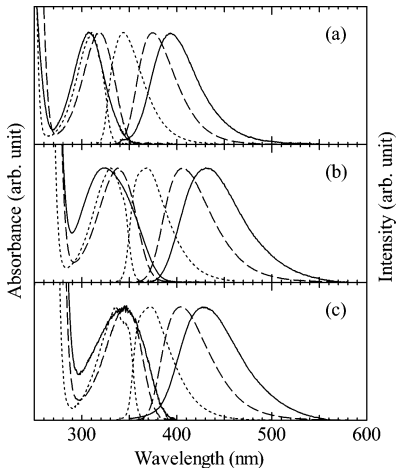

Figure 5. Absorption and fluorescence spectra of (a) *m*-ANCN, (b) *m*-DMCN, and (c) *m*-DECN in CH (···), MeCN (---), and H_2O (—).

It can therefore be concluded that the extreme fluorescence quenching of *m*-ANCN in water is related to the conformational change of the amino group in the S_1 state and variation in specific solute−solvent interactions upon electronic excitation. Figure 4 schematically illustrates the excited-state deactivation pathways of *m*-ANCN in aprotic solvent and in water. The significant structural change of the solute molecule and the variation in the solvation upon electronic excitation would increase the Franck−Condon factor for the $S_1(\pi\pi^*) \rightarrow S_0$ radiationless transition. As a possible mechanism for the anomalously fast internal conversion of *m*-ANCN in water, a conical intersection between the $S_1(\pi\pi^*)$ and a repulsive excited state (shown by the broken line in Figure 4) can be invoked. Recently, Sobolewski and co-workers[57,58] have suggested from MO theoretical calculations that in aromatic biomolecules such as nucleic bases and aromatic amino acids, a $^1\pi\sigma^*$ potential energy function intersects the bound potential energy function of the ground state, resulting in very fast internal conversion. For aniline a 3s-Rydberg or $^1\pi\sigma^*$ state is predicted to lie between the first and second valence states.[59,60] Such a polar excited state would have the possibility to intersect with the lowest $^1\pi\pi^*$ state in a polar environment such as in water, resulting in ultrafast internal conversion through $^1\pi\sigma^*-S_0$ conical intersection. The stronger quenching ability of water relative to TFE can thus be explained by the difference in polarity.

3.4. Possible Application as a Protein Probe. Figure 5 shows the absorption and fluorescence spectra of *m*-ANCN, *m*-DMCN, and *m*-DECN in CH, MeCN, and H_2O. By changing solvent from water to CH and MeCN, the absorption bands are shifted to the red (except for *m*-DECN) and the fluorescence bands shift to the blue. The fluorescence band position of these compounds depends strongly on the polarity of the solvent. The first absorption and fluorescence maximum and photophysical parameters of *m*-DMCN and *m*-DECN are presented in Table 4. As a result of *N*-alkylation, both the absorption and fluorescence spectra are found to be remarkably red shifted as compared with *m*-ANCN (see Figure 5 and Tables 2 and 4). The fluorescence quantum yield and lifetime of *m*-DMCN and *m*-DECN in CH, MeCN, and EtOH are relatively large ($\Phi_f > 0.1$) and much larger than those of *m*-ANCN because of the smaller k_{nr} of *m*-DMCN and *m*-DECN in these solvents (see Tables 2 and 4). In H_2O the magnitude of Φ_f and τ_f becomes extremely small in a similar manner as for *m*-ANCN.

As described above, *m*-DMCN and *m*-DECN are highly fluorescent in nonaqueous environments, while they are very weakly fluorescent in aqueous environment. The first absorption maxima have relatively large extinction coefficients (2750 M^{-1} cm^{-1} for *m*-DMCN and 2840 M^{-1} cm^{-1} for *m*-DECN in EtOH) and appear at wavelengths longer than 330 nm in hydrophobic solvents. This enables us to selectively excite these compounds in protein suspensions even when the proteins contain fluorescent amino acid residues (tryptophan, tyrosine, and phenylalanine[13]). In addition, the fluorescence bands of *m*-DMCN and *m*-DECN appear in the blue region of the visible spectrum ($\lambda > 400$ nm), and the fluorescence maximum depends strongly on the solvent polarity. One of the most important characteristics of a fluorescent probe based on intensity parameter, for hydrophobic domains of organized biological systems such as a protein, is that the probe molecule should be nonfluorescent in water but should show significant enhancement of fluorescence intensity when the molecule partitions to hydrophobic environments. In addition, the spectral features of the probe should permit clear wavelength windows for excitation and fluorescence in the presence of intrinsic fluorescence of the system under study. Characteristic photophysical properties of *m*-DMCN and *m*-DECN appear to satisfy these basic considerations. Some preliminary fluorescence spectral studies of the interaction of these molecules with the protein Human Serum Albumin (HSA) were carried out.

HSA was chosen as a representative protein because it is known to have hydrophobic binding sites and it has been one of the most extensively studied of all the proteins.[61] HSA is

TABLE 4: Photophysical and Spectral Properties of *m*-DMCN and *m*-DECN in Organic Solvents and H_2O at 293 K

compd	solvent	λ_{max}^{abs}/nm	λ_{max}^{fluo}/nm	$\Delta\bar{\nu}/10^3$ cm^{-1}	Φ_f	τ_f/ns	$k_f/10^7$ s^{-1}	$k_{nr}/10^8$ s^{-1}
m-DMCN	CH	331	369	3.11	0.19	3.7	5.2	2.2
	MeCN	339	407	4.93	0.69	27	2.6	0.11
	EtOH	339	412	5.23	0.59	23	2.5	0.18
	H_2O	324	432	7.72	0.003	0.26	1.3	39
m-DECN	CH	336	373	2.95	0.11	4.2	2.7	2.1
	MeCN	346	405	4.21	0.66	26	2.5	0.13
	EtOH	345	410	4.60	0.56	23	2.4	0.19
	H_2O	345	429	5.68	0.004	0.33	1.2	30

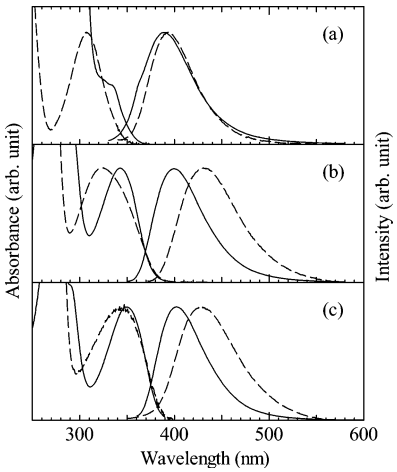

Figure 6. Absorption and fluorescence spectra of (a) *m*-ANCN, (b) *m*-DMCN, and (c) *m*-DECN in H_2O (---) and in HSA (—). [HSA] = 5×10^{-5} M, [*m*-cyanoanilines] = 5×10^{-5} M.

TABLE 5: Fluorescence Lifetime of *m*-Cyanoanilines in HSA[a]

compd	λ_{exc}/nm	λ_{em}/nm	τ_1/ns	τ_2/ns	χ^2
m-ANCN	320	390	1.42 (69)	8.77 (31)	1.27
m-DMCN	340	400	5.16 (35)	20.2 (65)	1.11
m-DECN	340	400	6.06 (26)	21.9 (74)	1.13

[a] [HSA] = 5.0×10^{-5} M, [*m*-cyanoanilines] = 5.0×10^{-5} M.

one of the most abundant proteins in the circulatory system and plays a key role in the transport of various substances. It has a remarkable ability to bind a wide variety of metabolites, toxins, and pharmaceuticals. With addition of HSA to the solution of *m*-ANCN, *m*-DMCN, and *m*-DECN in H_2O, the fluorescence intensity increased dramatically (by a factor of about 80 for *m*-DMCN and *m*-DECN under the presence of HSA (5×10^{-5} M)), and the absorption and fluorescence spectra shifted to the opposite directions under the presence of HSA (see Figure 6). Such remarkable changes in fluorescence intensity and spectral positions demonstrate that these molecules are incorporated in the hydrophobic site(s) of HSA. This is complemented by the fluorescence lifetime data shown in Table 5. Under the presence of HSA (5×10^{-5} M) in H_2O, the fluorescence lifetimes of *m*-ANCN, *m*-DMCN, and *m*-DECN increase drastically and the fluorescence decays conform to double exponential functions with lifetimes and relative amplitudes as shown in Table 5. A simple explanation for the finding of two different lifetime components in HSA is obtained if one assumes that the *m*-cyanoanilines are incorporated into at least two different binding sites in HSA. The extremely short lifetime components as observed in H_2O are not seen under the presence of HSA, which indicates that almost all *m*-cyanoanilines molecules are incorporated under this condition. The absorption and fluorescence band positions of *m*-DMCN and *m*-DECN in HSA are close to those in MeCN (see Figures 5 and 6), suggesting that apparent polarity of the binding site(s) is comparable to that of acetonitrile.

The fluorescence response of *m*-DMCN and *m*-DECN in HSA suspensions in terms of intensity enhancement, spectral shift, and fluorescence lifetime enhancement clearly suggests that these molecules are good candidates for further investigations as fluorescent molecular probes for hydrophobic domains of proteins. In addition, since the molecular size of *m*-cyanoanilines is much smaller than the usual sizes of fluorescent probe molecules,[13−15] they can be used without significant perturbation to intrinsic structures of biological substances.

Acknowledgment. This work was partly supported by a Grant-in-Aid from the Ministry of Education, Science, Sports, and Culture of Japan. A.K.M. acknowledges a Visiting Scientist Fellowship from the Japan Society for the Promotion of Sciences (JSPS).

References and Notes

(1) Jones, G., II; Jackson, W. R.; Choi, C.; Halpern, M. A. *Chem Phys. Lett*. **1980**, *72*, 391.
(2) Jones, G., II; Jackson, W. R.; Choi, C.; Bergmark, W. R. *J. Phys. Chem.* **1985**, *89*, 294.
(3) Van Gompel, J. A.; Schuster, G. B. *J. Phys. Chem.* **1989**, *93*, 1292.
(4) Arbeloa, T. L.; Arbeloa, F. L.; Tapia, M. J.; Arbeloa, I. L. *J. Phys. Chem.* **1993**, *97*, 4704.
(5) Seixas de Melo, J. S.; Becker, R. S.; Maçanita, A. L. *J. Phys. Chem.* **1994**, *98*, 6054.
(6) Raju, B. B.; Varadarajan, T. S. *J. Phys. Chem.* **1994**, *98*, 8903.
(7) Gustavsson, T.; Cassara, L.; Gulbinas, V.; Gurzadyan, G.; Mialocq, J.-C.; Pommeret, S.; Sorgius, M.; van der Meulen, P. *J. Phys. Chem. A* **1998**, *102*, 4229.
(8) Raju, B. B.; Costa, S. M. B. *Phys. Chem. Chem. Phys*. **1999**, *1*, 3539.
(9) Azuma, K.; Suzuki, S.; Uchiyama, S.; Kajiro, T.; Santa, T.; Imai, K. *Photochem. Photobiol. Sci*. **2003**, *2*, 443.
(10) Vogel, M.; Rettig, W.; Sens, R.; Drexhage, K. H. *Chem. Phys. Lett*. **1988**, *147*, 452.
(11) Arbeloa, F. L.; Arbeloa, T. L.; Gil Lage, E.; Arbeloa, I. L.; De Schryver, F. C. *J. Photochem. Photobiol.* **1991**, *56*, 313.
(12) Arbeloa, F. L.; Arbeloa, T. L.; Tapia Estévez, M. J.; Arbeloa, I. L. *J. Phys. Chem.* **1993**, *97*, 4704.
(13) Lakowicz, J. R. *Principles of Fluorescence Spectroscopy*, 2nd ed.; Kluwer Academic/Plenum: New York, 1999.
(14) Valeur, B. *Molecular Fluorescence*; Wiley-VCH: Weinheim, Germany, 2002.
(15) Hof. M.; Hutterer, R.; Fidler, V., Eds. *Fluorescence Spectroscopy in Biology*; Springer Series on Fluorescence 3; Springer-Verlag: Berlin, Germany, 2004.
(16) Weber, G.; Laurence, D. J. R. *Biochem. J*. **1954**, *56*, 31P.
(17) Weber, G.; Farris, F. J. *Biochemistry* **1979**, *18*, 3075.
(18) Shobini, J.; Mishra, A. K. *Spectrochim. Acta, Part A* **2000**, *56A*, 2239.
(19) Debnath, D. K.; Mukhopadhyay, K.; Basak, S. *Biophys. Chem*. **2005**, *116*, 159.
(20) Fleming, G. R.; Porter, G.; Robbins, R. J.; Synowiec, J. A. *Chem. Phys. Lett*. **1977**, *52*, 228.
(21) Sadkowski, P. J.; Fleming, G. R. *Chem. Phys*. **1980**, *54*, 79.
(22) Robinson, G. W.; Robbins, R. J.; Fleming, G. R.; Morris, J. M.; Knight, A. E. W.; Morrison, R. J. S. *J. Am. Chem. Soc.* **1978**, *100*, 7145.
(23) Seliskar, C. J.; Brand, L. *J. Am. Chem. Soc.* **1971**, *93*, 5405.
(24) Seliskar, C. J.; Brand, L. *J. Am. Chem. Soc.* **1971**, *93*, 5414.
(25) Kosower, E. M.; Dodiuk, H.; Kanety, H. *J. Am. Chem. Soc*. **1978**, *100*, 4179.
(26) Kosower, E. M.; Kanety, H. *J. Am. Chem. Soc.* **1983**, *105*, 6236.
(27) Kitamura, N.; Sakata, N.; Kim, H.-B.; Habuchi, S. *Anal. Sci*. **1999**, *15*, 413.
(28) Förster, T.; Rokos, K. *Chem. Phys. Lett*. **1967**, *1*, 279.
(29) Detoma, R. P.; Brand, L. *Chem. Phys. Lett*. **1977**, *47*, 231.
(30) Ebbesen, T. W.; Ghiron. C. A. *J. Phys. Chem*. **1989**, *93*, 7139.
(31) Vázquez, M. E.; Nitz, M.; Stehn, J.; Yaffe, M. B.; Imperiali, B. *J. Am. Chem. Soc.* **2003**, *125*, 10150.
(32) Lobo, B. C.; Abelt, C. J. *J. Phys. Chem. A* **2003**, *107*, 10938.
(33) Davis, B. N.; Abelt, C. J. *J. Phys. Chem. A* **2005**, *109*, 1295.
(34) Tajima, S.; Shiobara, S.; Shizuka, H.; Tobita, S. *Phys. Chem. Chem. Phys*. **2002**, *4*, 3376.
(35) Shiobara, S.; Kamiyama, R.; Tajima, S.; Shizuka, H.; Tobita,S. *J. Photochem. Photobiol. A* **2002**, 154, 53.
(36) Shiobara, S.; Tajima S.; Tobita, S. *Chem. Phys. Lett*. **2003**, *380*, 673.
(37) Srivastava, S. K.; Chauhan, P. M. S.; Bhaduri, A. P. *Synth. Commun*. **1999**, *29*, 2085.
(38) Eaton, D. F. *Pure Appl. Chem*. **1988**, *60*, 1107.
(39) Perichet, R. G.; Chaperon, R.; Pouyet, B. *J. Photochem*. **1980**, *13*, 67.
(40) Tajima, S.; Tobita, S.; Shizuka, H. *J. Phys. Chem. A* **2000**, *104*, 11270.
(41) Dean, J. H., Ed. *Lange's Handbook of Chemistry*; McGraw-Hill: New York, 1973.
(42) Hansch, C.; Leo, A.; Taft, R. W. *Chem. Rev*. **1991**, *91*, 165.
(43) Taft, R. W.; Kamlet, M. J. *J. Am. Chem. Soc.* **1976**, *98*, 2886.
(44) Kamlet, M. J.; Abboud, J.-L.; Abraham, M. H.; Taft, R. W. *J. Org. Chem*. **1983**, *48*, 2877.

(45) Othmen K.; Boule, P.; Richard, C. *New J. Chem*. **1999**, *23*, 857.
(46) Freccero, M.; Fagnoni, M.; Albini, A. *J. Am. Chem. Soc.* **2003**, *125*, 13182.
(47) Druzhinin, S. I.; Jiang, Y.-B.; Demeter, A.; Zachariasse, K. A. *Phys. Chem. Chem. Phys*. **2001**, *3*, 5213.
(48) Braslavsky, S. E.; Heibel, G. E. *Chem. Rev*. **1992**, ***92***, 1381.
(49) Braslavsky, S. E.; Heihoff, K. In *Handbook of Organic Photochemistry*; Scaiano, J. C., Ed.; CRC Press: Boca Raton, FL, 1989; Vol. 1, pp 327−355.
(50) Saito, F.; Tobita, S.; Shizuka, H. *J. Chem. Soc., Faraday Trans*. **1996**, *92*, 4177.
(51) Saito, F.; Tobita, S.; Shizuka, H. *J. Photochem. Photobiol. A, Chem.* **1997**, *106*, 119.
(52) Suppan, P.; Ghoneim, N. *Solvatochromism*; Royal Society of Chemistry: Cambridge, UK, 1997.
(53) Tobita, S.; Ida, K.; Shiobara, S.; Shizuka, H. *Res. Chem. Inetermed.* **2001**, *27*, 205.
(54) Schuddeboom, W.; Jonker, S. A.; Warman, J. M.; Leinhos, U.; Kühnle, W.; Zachariasse, K. A. *J. Phys. Chem.* **1992**, *96*, 10809.
(55) Korter, T. M.; Borst, D. R.; Butler, C. J.; Pratt, D. W. *Chem. Phys. Lett*. **2001**, *123*, 96.
(56) Meek, J. T.; Sekreta, E.; Wilson, W.; Viswanathan, K. S.; Reilly, J. P. *J. Chem. Phys*. **1985**, *82*, 1741.
(57) Sobolewski, A. L.; Domcke, W.; Dedonder-Lardeux, C.; Jouvet, C. *Phys. Chem. Chem. Phys*. **2002**, *4*, 1093.
(58) Perun, S.; Sobolewski, A. L.; Domcke, W. *Chem. Phys*. **2005**, *313*, 107.
(59) Honda, Y.; Hada, M.; Ehara, M.; Nakatsuji, H. *J. Chem. Phys*. **2002**, *117*, 2045.
(60) Ebata, T.; Minejima, C.; Mikami, N. *J. Phys. Chem. A* **2002**, *106*, 11070.
(61) He, X. M.; Carter, D. C. *Nature* **1992**, *358*, 209.